Optically tuned resonant optical reflectance filter

Fuchyi Yang,[1] Gary Yen,[1] Gilles Rasigade,[1] Julio A. N. T. Soares,[2] and Brian T. Cunningham[1,a)]
[1]*Nano Sensors Group, Micro and Nanotechnology Laboratory, Department of Electrical and Computer Engineering, University of Illinois of Urbana-Champaign, 208 N. Wright Street, Urbana, Illinois 61801, USA*
[2]*Frederick Seitz Materials Research Laboratory, 104 S. Goodwin Avenue, Urbana, Illinois 61801, USA*

(Received 15 January 2008; accepted 12 February 2008; published online 5 March 2008)

We describe the design, fabrication, and characterization of a narrow band tunable guided mode resonance (GMR) reflectance filter that is actuated by optically induced *trans-cis* isomerization of an azobenzene liquid crystal. Constructing a plastic replica-molded containment cell with a rubbed polyimide film to initially direct the liquid crystal molecular orientation parallel to the grating lines of the GMR filter, isomerization caused by exposure to a $\lambda=532$ nm laser results in a −25 nm shift of the resonant reflected wavelength. © *2008 American Institute of Physics*. [DOI: 10.1063/1.2890713]

Guided mode resonant (GMR) filters represent a novel and a unique class of reflectance filters that are capable of reflecting a narrow resonant band of wavelengths with nearly 100% efficiency for wavelengths spanning from UV[1] to IR.[2–7] GMR filters can exhibit the same bandwidth and reflection efficiency as multilayer Bragg filters, but can be fabricated using a one-dimensional (1D) or two-dimensional periodic grating structure combined with a single high refractive index thin film deposition using either lithography[8,9] or plastic-based replica molding[10,11] to form the required subwavelength grating structure. Since the demonstration of the first static GMR filters,[12,13] efforts have been made to incorporate materials with variable refractive index that can be controlled either optically[14] or electrically[15–19] that can result in a filter with properties that are tunable. Applications for tunable filters include laser eye protection, optical limiting for sensor protection,[20] optical switching, video display, and optical memory, where selective opening or closing of an optical passband can be utilized. Suitability of tunable GMRs for these applications will be determined by the extent of wavelength tuning, tuning speed, and the cost of efficiently fabricating GMRs over large surface areas.

In this work, we describe the design, fabrication, and characterization of a tunable GMR in the visible wavelength range that is fabricated with a plastic-based nanoreplica molding process on flexible substrates that incorporates an azobenzene liquid crystal (azo-LC) as a variable refractive index material that is actuated by exposure to a pump laser beam. A −25 nm resonant wavelength shift is obtained that maintains its state after the pump laser is turned off.

Azobenzene liquid crystals are a unique class of material that incorporate novel features from both liquid crystals and azobenzene molecules.[21] They have the long range ordering of liquid crystals, such as the nematic mesophase, while simultaneously exhibiting photo isomerization between *trans-* and *cis*-configurations typical of azobenzene molecules. Absorption of electromagnetic radiation at the correct wavelength range enables photo isomerization which changes the refractive index properties of the bulk material.

a)Author to whom correspondence should be addressed. Electronic mail: bcunning@uiuc.edu.

The device cross section schematic is shown in Fig. 1. A 1D periodic grating is produced using UV-cured polymer (UVCP) material on a polyethylene terephthalate (PET) substrate. A thin film layer of titanium dioxide (TiO_2) is deposited over the UVCP grating. Facing the grating structure from above is an upper PET substrate containing a replicated spacer that sets the gap distance between the grating structure and the upper substrate, and polyimide (PI) film for liquid crystal alignment. The two PET substrates are hermetically sealed creating an empty cavity into which azo-LC material is subsequently injected. In this letter, the z direction is vertical to the device substrate, the x direction refers to the direction perpendicular to the grating lines, and the y direction is parallel to the grating lines as shown. Light is incident upon the structure from the bottom, propagating in the $+z$ direction with its electric field parallel to the grating lines (TE mode). At the resonant wavelength for TE illumination, an optical standing wave develops with its electric field oriented in the y direction. The wavelength of resonant reflection is referred to as the peak wavelength value (PWV). The rubbed PI film homogeneously aligns the azo-LC parallel to the grating lines. Exposing the azo-LC to 532 nm illumina-

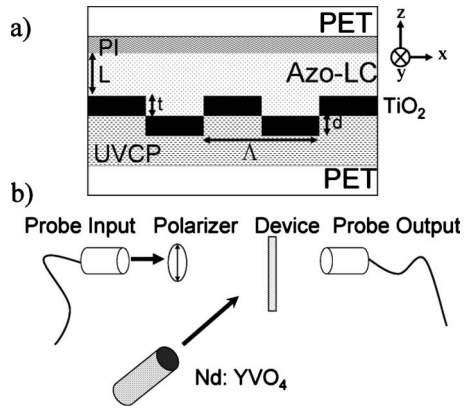

FIG. 1. (a) A cross section schematic view of the device is shown. The grating period is $\Lambda=370$ nm with a height of $d=55$ nm. The TiO_2 thickness is $t=90$ nm and the LC cell is $L=5$ μm thick. (b) The experimental pump probe diagram is illustrated. Incident light (broadband or HeNe laser) travels through a polarizer and illuminates the device. The transmitted light is coupled to a spectrometer or photodiode. A cw $Nd:YVO_4$ pump laser is used.

tion will induce photoisomerization from *trans* to *cis*. This change causes a decrease in the refractive index of the azo-LC layer along the *y* direction. As a result, the TE PWV will shift to shorter wavelength values.

The resonance filter was fabricated by employing a nanoreplica molding process using a silicon "master" wafer as a mold template. The silicon master is an 8-in.-diameter wafer upon which a linear grating structure with a period of 370 nm and a ~50% duty cycle is patterned by deep-UV photolithography over an $\sim 5 \times 5$ in.^{2} area. The grating pattern is etched into the silicon wafer to a depth of 70 nm by reactive ion etching. A layer of liquid acrylate UVCP was drop coated on top of the silicon master. The PET substrate is then placed over the silicon master, and is then pressed over the master using a rolling cylinder. This enables the UVCP drops to form a thin continuous layer between the two surfaces and conform to the features of the master. After this has been achieved, the UVCP is cured using a UV lamp for 90 s. Next, the PET substrate is released from the master and a cured UVCP layer with a period of $\Lambda = 370$ nm and a duty cycle of ~50% is replicated on the PET substrate. Subsequently, TiO_2, serving as the high index layer, was deposited on top of this UVCP layer by e-beam evaporation with a thickness of 90 nm. The same nanoreplica molding method is used to fabricate spacers on the top PET substrate but using a different silicon master with appropriate features. The spacer consists of a frame designating the boundary of the LC cell and support posts evenly spaced within the frame to prevent sagging and to maintain a constant height of 5 μm. A polyimide, PI-2556 (HD Microsystems), film is spin coated over the spacer and then baked and rubbed with a velvet cloth. Holes are created through the upper PET substrate for azo-LC injection. The LC cell is then completed by sealing the two PET substrates. To accomplish this, the two substrates are clamped together using magnets on both sides. The PI film's rubbed direction is aligned parallel with the direction of the grating lines. Then, UV-curable optical bonding adhesive (SK9, Summers Optical) is applied around the border of the frame and cured. After sealing of the LC cell, roughly 5 μl of azo-LC, 1005 (BEAM Corp.), is injected into the cell through the holes using a pipette.

The tuning of the optical reflectance filter is characterized using the pump/probe setup shown in Fig. 1. A transmission setup is used to probe the device, while a cw $Nd:YVO_4$ laser serves as the pump source. An optical fiber and collimator lens illuminates the device with broadband light through a linear polarizer such that only the TE mode is excited. The transmitted light is collected using a second optical fiber connected at its distal end to a spectrometer (Ocean Optics) that is interfaced to a computer. The spectrum has a transmission minimum at the PWV corresponding to a reflectance maximum. The transmission efficiency is below 10%, indicating at least 90% reflection efficiency. The PWV is initially at $\lambda = 660.74$ nm. After pumping the device with the $Nd:YVO_4$ laser at 30 mW output power and 1 cm beam diameter, the PWV shifts to $\lambda = 635.35$ nm, as shown in Fig. 2, for a difference of $\Delta\lambda = 25.39$ nm.

A time curve is shown in Fig. 3, depicting the temporal change of the PWV using 30 mW pump laser. To achieve this, a 1 mW HeNe laser is used to probe the device at oblique incidence. Since the PWV is sensitive to the angle of incidence of incoming light, it is possible to shift the PWV so that it spectrally overlaps with the 632 nm emission line of the HeNe laser. A Si photodiode is placed at output end of the device to collect the transmitted 632 nm light. The photodiode is connected to an oscilloscope and the data are recorded using a custom LABVIEW program. Initially, most of the 632 nm light is transmitted by the device and a maximum signal is observed from the photodiode. When the pump laser is turned on, the PWV shifts and spectrally overlaps with the 632 nm light. Thus, the light from the HeNe is blocked by the device, and the photodiode signal decreases and stabilizes at ~0 V, as shown in Fig. 3. From the data, the response time of the device is 80 ms and the contrast ratio between on and off values is 100:1. The contrast ratio corresponds to a reflection efficiency of at least 99% for the reflectance filter. In addition, the time dependence of the PWV shift on the pump laser power was investigated. A continuously variable neutral density filter was placed in front of the pump laser, and a Si power meter was used to measure the amount of pump power incident on the device. Figure 3 (inset) illustrates that the time it takes for the PWV to shift decreases nonlinearly with increasing pump power. The spectral change of the HeNe laser transmission was also observed by replacing the photodiode with a spectrometer as previously described. Figure 4 shows the initial spectrum of the laser with a reduced transmitted intensity at 632 nm due to the PWV. Notice that the HeNe laser also has an emission line at 612 nm. This emission wavelength is initially allowed to pass. After the filter is pumped with the 532 nm laser, the PWV shifts to 612 nm and blocks that wavelength while allowing the 632 nm light to transmit.

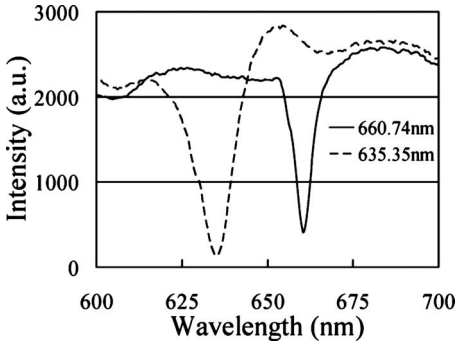

FIG. 2. Transmission spectrum illustrating TE PWV shift. The initial (solid) and final (dotted) spectra indicate a shift of −25.39 nm due to *trans-cis* photoisomerization of azo-LC. The transmission efficiency is below 10%.

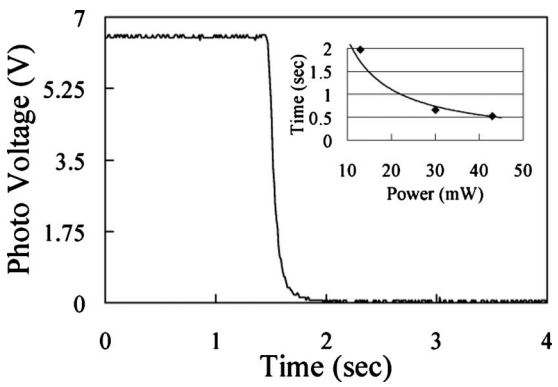

FIG. 3. Time response measurement of PWV shift. The transmitted light decreases intensity due to the PWV shifting toward 632 nm. The inset shows the time response dependence on pump laser power.

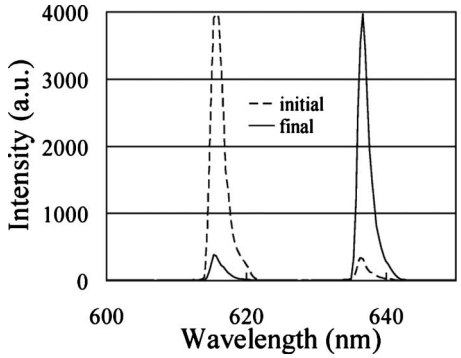

FIG. 4. Transmission spectra of a HeNe laser before and after PWV tuning. Initial reflection of the 632 nm line is transmitted after *trans-cis* photoisomerization of the azo-LC.

The time response is determined by the mechanism by which the azo-LC undergoes photoisomerization upon exposure to 532 nm radiation. Absorption of the pump laser light by the azo-LC molecules changes their phase from nematic (*trans*) to isotropic (*cis*). Thus, the refractive index of the azo-LC layer changes which shifts the PWV. The azo-LC director is initially along the grating lines due to the rubbed PI film. Thus, the refractive index is $n_{\|}=1.726$. After photoisomerization, the refractive index is $n_{cis}=1.57$, resulting in a negative refractive index change of $\Delta n=n_{cis}-n_{\|}=-0.156$. This refractive index change causes the PWV to shift to shorter wavelength values. This behavior is consistent with simulations done using rigorous coupled wave analysis software (DIFFRACT MOD, Rsoft). The results are not shown here but similar results were discussed in a previous publication.[18]

The isotropic cis state of the particular azo-LC material used in this report is relatively stable.[22] By observing the PWV of a device over time, it was determined that 24 h was required for the azo-LC to relax back to its nematic trans state when left in a dark environment. This relaxation process was speed up by heating the device in an oven at 65 °C for 30 min and allowed to cool back to room temperature.

The optical switching properties of azo-LC materials continue to be an area of intense research, as novel molecular structures are engineered to provide maximum absorption at particular wavelengths and rapid switching speed resulting from low pump illumination intensity.[22,23] Materials with rapidly reversible *cis*-to-*trans* transitions induced either spontaneously or through illumination with a laser have also been reported. In future work, we expect to incorporate alternative azo-LC into the GMR structure for demonstration of more rapid switching speed.

In conclusion, optical reflectance filters were fabricated on flexible substrates using nanoreplica molding. The reflected wavelength was optically tuned over 25 nm using a 532 nm cw laser. Tuning was achieved by incorporating a layer of azo-LC which changed its refractive index upon illumination of 532 nm radiation.

This research was supported by the U.S. Army (Project Manager Dr. Joel Carlson) under Contract No. W911QY-06-C-0043, and acknowledge Dr. Carlson for many helpful discussions.

[1]N. Ganesh and B. T. Cunningham, Appl. Phys. Lett. **88**, 071110 (2006).
[2]M. Neviere, P. Vincent, R. Petit, and M. Cadilhac, Opt. Commun. **9**, 48 (1973).
[3]A. Hessel and A. A. Oliner, Appl. Opt. **4**, 1275 (1965).
[4]L. F. Desandre and J. M. Elson, J. Opt. Soc. Am. A Opt. Image Sci. Vis **8**, 763 (1991).
[5]P. C. Mathias, N. Ganesh, L. L. Chan, and B. T. Cunningham, Appl. Opt. **46**, 2351 (2007).
[6]I. D. Block, L. L. Chan, and B. T. Cunningham, Sens. Actuators B **120**, 187 (2006).
[7]N. Ganesh, A. Xiang, N. B. Beltran, D. W. Dobbs, and B. T. Cunningham, Appl. Phys. Lett. **90**, 081103 (2007).
[8]Z. S. Liu, S. Tibuleac, D. Shin, P. P. Young, and R. Magnusson, Opt. Lett. **23**, 1556 (1998).
[9]R. Magnusson, D. Shin, and Z. S. Liu, Opt. Lett. **23**, 612 (1998).
[10]B. Cunningham, J. Qiu, P. Li, and B. Lin, Sens. Actuators B **87**, 365 (2002).
[11]B. Cunningham, B. Lin, J. Qiu, P. Li, J. Pepper, and B. Hugh, Sens. Actuators B **85**, 219 (2002).
[12]L. Mashev and E. Popov, Opt. Commun. **55**, 377 (1985).
[13]I. A. Avrutsky and V. A. Sychugov, J. Mod. Opt. **36**, 1527 (1989).
[14]D. W. Dobbs and B. T. Cunningham, Appl. Opt. **45**, 7286 (2006).
[15]M. Haurylau, S. P. Anderson, K. L. Marshall, and P. M. Fauchet, IEEE J. Sel. Top. Quantum Electron. **12**, 1527 (2006).
[16]T. Katchalski, G. Levy-Yurista, A. A. Friesem, G. Martin, R. Hierle, and J. Zyss, Opt. Express **13**, 4645 (2005).
[17]A. Sharon, D. Rosenblatt, A. A. Friesem, H. G. Weber, H. Engel, and R. Steingrueber, Opt. Lett. **21**, 1564 (1996).
[18]F. Yang, G. Yen, and B. T. Cunningham, Appl. Phys. Lett. **90**, 261109 (2007).
[19]A. S. P. Chang, K. J. Morton, H. Tan, P. F. Murphy, W. Wu, and S. Y. Chou, IEEE Photonics Technol. Lett. **19**, 1457 (2007).
[20]M. J. Grout, Opt. Mater. (Amsterdam, Neth.) **14**, 155 (2000).
[21]U. Hrozhyk, S. Serak, N. Tabiryan, and T. J. Bunning, Mol. Cryst. Liq. Cryst. **454**, 235 (2006).
[22]N. Tabiryan, U. Hrozhyk, and S. Serak, Phys. Rev. Lett. **93**, 113901 (2004).
[23]S. V. Serak, N. V. Tabiryan, M. Peccianti, and G. Assanto, IEEE Photonics Technol. Lett. **18**, 1287 (2006).